

The Radial Electric Field of MAST

D. Temple^{1,2}, H. Meyer², A. Kirk², E. Nardon² and the MAST and NBI teams²

¹Imperial College Plasma Physics Group, Blackett Laboratory, London, SW7 2AZ, U.K.

²EURATOM / UKAEA Fusion Association, Culham Science Centre, OX14 3DB, U.K.

This work was funded jointly by the United Kingdom Engineering and Physical Sciences Research Council and by the European Communities under the contract of association between EURATOM and UKAEA. The views and opinions expressed herein do not necessarily reflect those of the European Commission

Background

Magnetically-confined plasmas may undergo a transition from a state of lower confinement (L-mode) to one of higher confinement (H-mode) [1], the latter having higher core densities and temperatures and so a greater fusion yield per unit volume. H-mode plasmas are therefore more attractive for the prospect of commercial fusion energy, and understanding this phenomenon is important for fusion research.

The H-mode state is thought to arise as a consequence of self-organised processes acting to retain radial equilibrium of forces. The main components of this momentum-balance are the radial pressure gradient, the radial electric field and the Lorentz force from perpendicular motion, so for the steady state of some species s we require that :-

$$\mathbf{F}_{r,s} = -\frac{1}{n_s} \frac{\partial p_s}{\partial r} \hat{\mathbf{r}} + q_s (E_r + \mathbf{v}_s \times \mathbf{B} \cdot \hat{\mathbf{r}}) \hat{\mathbf{r}} = 0 \quad (1)$$

Strong radial shear of flows in the $\mathbf{E}_r \times \mathbf{B}$ direction exists in the edge of H-mode plasmas [2], arising due to a sheared E_r which must arise as a consequence of balancing the other terms of equation (1). Turbulent vortices are radially distorted and de-correlated by this flow-shear, resulting in an edge-transport-barrier (ETB) that restricts radial outflow [3]. The L-H transition is a highly non-linear process; the increased confinement of the H-mode steepens the edge pressure profile, which then affects the edge E_r and so the $\mathbf{E}_r \times \mathbf{B}$ flow shear which gave the increased confinement in the first place, and so on.

Transport barriers due to sheared $\mathbf{E}_r \times \mathbf{B}$ motion can occur throughout the plasma, but conditions in the edge are such that this is a particularly favourable location. Here we typically have the steepest pressure gradients regardless of the state of confinement, and the high magnetic shear means that any flow gives a sheared perpendicular component to flows at neighbouring radial points by viscous transfer. In the edge plasma there is such viscous transfer due to both scrape-off-layer flows and core rotation, giving a dual momentum input to the intermediate region.

There is currently no predictive theory to explain all the complex physics of the edge plasma, which is key to understanding the L-H transition, and more experimental work is needed. Recent investigations on MAST have focused on the time-evolution of E_r over the course of H-mode plasmas, and the effect of resonant-magnetic-perturbations (RMPs) being investigated for their potential to mitigate edge-localised-modes (ELMs), which are an inherent and detractive aspect of the H-mode. Our results are therefore significant not only for spherical tokamaks but to magnetically-confined plasmas in general.

Measuring E_r in MAST

Re-arranging equation (1) for E_r and expanding terms, we have the following :-

$$\mathbf{E}_r = T_s \frac{q_e}{q_s} \left(\frac{\partial \ln n_s}{\partial r} + \frac{\partial \ln T_s}{\partial r} \right) \hat{\mathbf{r}} - (\mathbf{v}_s \times \mathbf{B} \cdot \hat{\mathbf{r}}) \hat{\mathbf{r}} \quad (2)$$

Where the temperature T_s is in eV . The terms of this equation for some radiating species s can be found by the technique of Doppler spectroscopy, and such a system (ECELESTE [4]) is used on MAST as shown in figure 1.

A concentrated source of the 468.57nm He_{II} emission line is given by a localised Helium gas jet into the low-field-side plasma edge, which is observed by 64 poloidal and 64 toroidal lines of sight focused through a Czerny-Turner spectrometer onto a frame-transfer CCD. A radial plasma view and a Zn lamp are used to provide reference wavelengths.

The integrated photon counts from each measured emission line are used with the ADAS atomic modelling data set, in conjunction with n_e and T_e profiles from Thomson scattering, to yield $\partial \ln(n_s)/\partial r$ profiles for the dominant ground-state He_{II}. Line widths and centroid Doppler shifts then provide the temperature and velocity profiles respectively, and magnetics data is given by EFIT equilibrium reconstruction to complete the set of ingredients needed to satisfy equation (2).

It is important to note that the individual terms of the radial force balance needn't be the same for all species; only the radial electric field is common. The separate He_{II} density, temperature and velocity profiles from ECELESTE hence aren't directly related to plasma quantities in absolute terms, only the relative changes are expected to correlate.

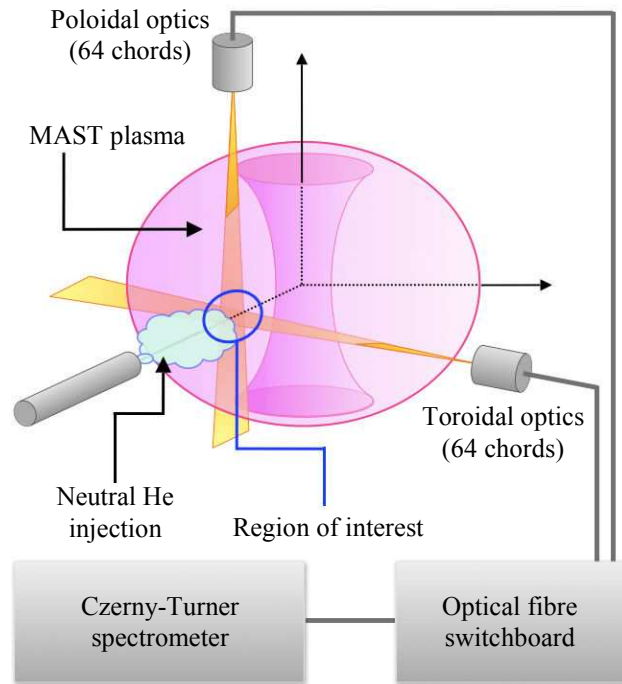


Figure 1: The ECELESTE diagnostic

Results and Discussion

Figure 2 shows ECELESTE edge E_r data from MAST shot #18571. From the divertor D_α signal in figure 2(a) it can be seen that the plasma entered the H-mode phase at ~ 0.210 s with ~ 100 Hz ELM frequency, subsequently developing into an ELM-free H-mode at ~ 0.350 s. The E_r data show a distinct correlation in profile evolution with these changes in confinement.

In figure 2(b) we see that the total field is relatively flat and positive at ~ 3 kV m^{-1} prior to the L-H transition, subsequently developing a bump-and-well feature in the outermost plasma and a slightly negative region further in. Figure 2(c) and (d) show the breakdown of the total field into the component He_{II} pressure and Lorentz terms of equation (2), respectively. It can be seen that the bump-and-well derive from the behaviour of the pressure term, with the positive bump sitting between $\psi_n=0.90$ and $\psi_n=0.95$ and the negative well between $\psi_n=0.95$ and $\psi_n=1.00$. The change in the total core profile is dominated by the behaviour of the Lorentz term, which is otherwise flat. In this case the plasma went through a dithery phase

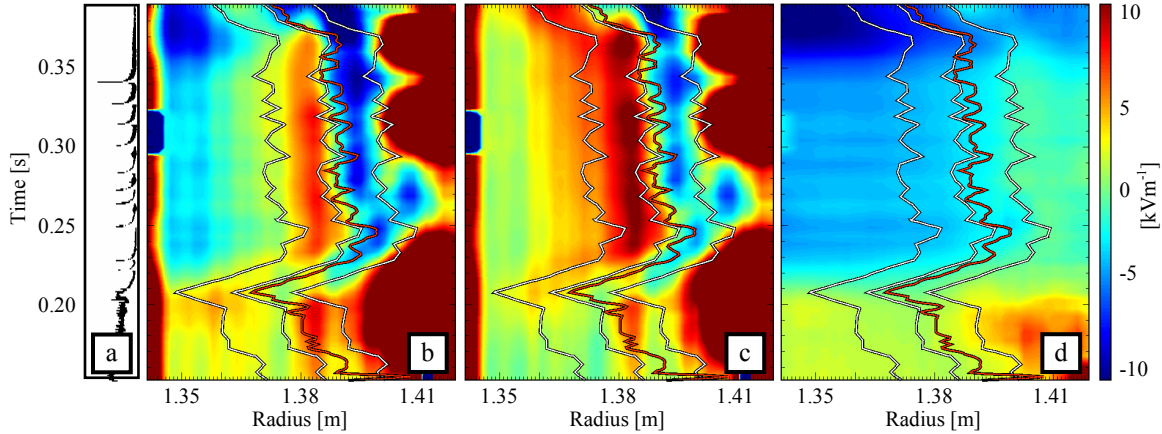


Figure 2: Evolution of E_r over MAST shot #18571. (a) Divertor D_α showing the L-H transition at ~ 0.210 s (b) E_r :Total (c) $He_{II}E_r$:Pressure (d) $He_{II}E_r$:Lorentz. Overlaid are lines showing ψ_n at 0.90, 0.95 and 1.00 in white, and the D_α peak radius in red. Areas of hard red and hard blue should be ignored.

before remaining in the higher confinement state, making it difficult to assess the influence of the edge E_r on the causality of the L-H transition itself.

The bump-and-well continue to evolve throughout the H-mode phase, with the well growing broader and deeper and the inner gradient increasing with time. This reveals that the expected region of sheared $\mathbf{E}_r \times \mathbf{B}$ velocity becomes larger and even more sheared, suggesting that the ETB actually grows and strengthens as the plasma develops. Thomson scattering readings of n_e and T_e show correlating increases in confinement, in agreement with this observation.

The Lorentz term is indicative of a distinct shift in the perpendicular plasma flow upon the L-H transition, which is steady during each of the separate confinement stages. Following the ELMy H-mode phase, as indicated by the periodic D_α spikes in figure 2(a), the Lorentz term dips to a more negative value in the core which spreads to greater radii with time. This reveals how perpendicular angular momentum is removed from the bulk plasma by ELMs, allowing the plasma to spin up in the quiescent phase.

Figure 3 shows the effect on E_r and plasma density given by the application of RMPs [5], where the strength of the perturbations is indicated by the current in the coils used to induce them (I_{RMP}). In all cases we observe an initial positive rise in E_r and a loss of plasma density for ~ 0.050 s from the time at which the perturbations are applied, but afterwards this behaviour is only sustained for $I_{RMP} > 1.0$ kA. This is suggestive of an I_{RMP} threshold for the perturbations to have a significant effect.

The current best theoretical picture for the action of RMPs is a two-stage process [6]. In the first stage a parallel current is induced by the RMPs and flux surfaces are distorted to include a radial B -field component, with the interaction of the two then providing a torque which acts to slow plasma rotation. This should lead to a more positive E_r through the Lorentz term.

In the second stage the damped rotation allows the perturbations to induce magnetic islands on rational flux surfaces, which grow until they overlap and create a stochastic field. A fast channel for particles to stream out of the plasma is thus created, so reducing density. A charge disparity is set up on either side of the last-closed-flux-surface as the more-mobile electrons initially stream from the plasma faster, giving a radial current that acts with the B -field to provide a further torque, again giving a positive contribution to the E_r Lorentz term. Our results are hence qualitatively supportive of this process, as are E_r data from reciprocating probe readings.

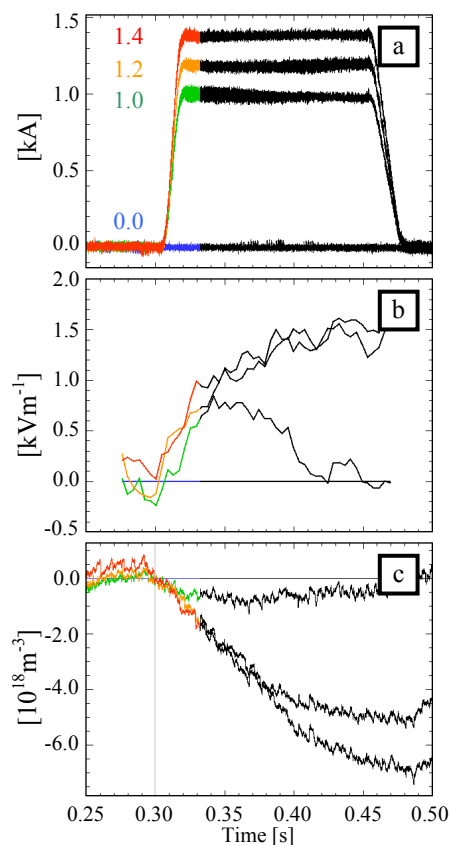


Figure 3: Effect of RMPs
 (a) RMP coil-current (I_{RMP})
 (b) Change* in E_r : Lorentz at $\psi_n=0.90$
 (c) Change* in plasma density
 *with respect to the $I_{RMP}=0$ plasma

It is noted for the $I_{RMP} = 1.0\text{kA}$ plasma that both the E_r rise and the density loss turn over at approximately the same time, which is also the point at which the $\partial E_r/\partial t$ is reduced in the highest two I_{RMP} cases. This could be interpreted as a reduction in E_r generation by the first stage RMP process from above at this time, possibly due to internal rotation-driving mechanisms countering the RMP-induced braking. In the $I_{RMP} = 1.0\text{kA}$ case this braking may be too weak to resist the rotational drive from taking over, which then reverses the E_r change and halts the B -field stochastisation from becoming fully established, quashing the density pump-out. The stochastisation may already be high in the greatest two I_{RMP} plasmas when the rotational drive picks up, such that the second-stage RMP process remains intact. This would explain the continued density loss and E_r rise, albeit with the latter now at a reduced rate due to the reduced first stage RMP process.

Comparing the plasmas with the highest two I_{RMP} we see little difference in the edge E_r yet a distinct difference in density pump-out. This suggests that the radial current due to the stochastic field causes a proportional and opposing current. The E_r would then be relatively constant even if stochastisation were to increase, yet the density loss would still be enhanced through the channel of ions and electrons being lost at the same rate.

The picture of plasma behaviour with applied RMPs does not seem to be complete, however. No correlation is seen between the application time or strength of the perturbations with the plasma temperature, for instance, which should be expected. Under closer inspection the E_r data from ECELESTE also suggest that an optimal I_{RMP} exists which is less than the maximum, which remains unexplained in the picture of increasing stochastisation with increasing I_{RMP} .

Conclusions

The edge E_r of MAST has been measured via Doppler spectroscopy with the ECELESTE diagnostic. Results show a distinct evolution of this field as plasma confinement changes, and a correlation of the widths of the ETB and a well feature in the E_r profile.

Work with RMPs suggests a threshold in the applied perturbation strength for proper effectiveness, and observations of the change in the edge E_r and plasma density qualitatively agree with theoretical expectations. Not all phenomena are completely explained, however, indicating a lack of understanding for some aspects of RMPs.

References

- [1] ASDEX Team, *Nuclear Fusion* **29** 1959-2040 (1989)
- [2] K. Burrell, *Physics of Plasmas* **4** (5) (1997)
- [3] P. Terry, *Reviews of Modern Physics* **72** (1) (2000)
- [4] H. Meyer et al, *Journal of Physics Conference Series* **123** 012005 (2008)
- [5] E. Nardon, *2009 EPS Plasma Physics Conference Invited Talk*
- [6] M.F.M. De Bock et al, *Nuclear Fusion* **48** 015007 (2008)